

Tensile Properties of $Zr_{70}Ni_{16}Cu_6Al_8$ BMG at Room and Cryogenic Temperatures

David D. E. Brennhaugen^{a,*}, Konstantinos Georgarakis^b, Yoshihiko Yokoyama^c, Koji S. Nakayama^d, Lars Arnberg^a and Ragnhild E. Aune^a

^a*Department of Materials Science and Engineering, NTNU, Norwegian University of Science and Technology, 7491 Trondheim, Norway*

^b*School of Aerospace, Transport and Manufacturing, Cranfield University, Cranfield MK43 0AL, UK*

^c*Institute for Materials Research, Tohoku University, 2-1-1, Katahira, Sendai 980-8577, Japan*

^d*New Industry Creation Hatchery Center, Tohoku University, 2-1-1, Katahira, Sendai 980-8577, Japan*

Abstract

The mechanical behaviour in tension of a hypoeutectic $Zr_{70}Ni_{16}Cu_6Al_8$ Bulk Metallic Glass (BMG) was studied at room (295K) and cryogenic temperatures (150 K and 77K) using various strain rates between 10^{-4} and $10^{-1} s^{-1}$. The yield strength was found to increase at lower temperatures with average values increasing by 16 %, from 1503 MPa at 295 K to 1746 MPa at 77 K. The Zr-based BMG was found to exhibit tensile plastic elongation of about 0.4% before fracture at room temperature and high strain rates ($10^{-1} s^{-1}$). Even higher tensile plasticity was recorded at low temperatures; plastic deformation was found highest at the intermediate temperature (150K) reaching remarkable plastic strains in the order of 3.9 %, while values up to 1.5% were recorded at 77 K. The lateral surface of the tensile specimens was observed in-situ during deformation using a high frame rate camera offering interesting insights with regard to the deformation mechanisms. Room temperature plasticity occurred through the formation and interaction of several nucleated shear bands before critical failure, while at intermediate and liquid nitrogen temperatures, most of the plastic deformation was accommodated through stable flow within a single shear band.

Keywords: amorphous materials, metallic glasses, mechanical properties

*Corresponding author: david.e.brennhaugen@ntnu.no

Introduction

Bulk Metallic Glasses (BMGs) exhibit a host of interesting and beneficial properties such as high mechanical strength, high hardness, high elastic limit as well as good wear and corrosion resistance, superior to that of conventional crystalline metals and alloys[1]. The bottleneck limiting the wider application of BMGs as structural materials relates, however, to their limited ductility, especially in tension. While BMGs often exhibit considerable plastic strains under compressive loads, most fail prematurely with very limited plastic deformation before fracture under tensile loading.

Understanding their precise mechanical behaviour and deformation mechanisms under tensile load is therefore very valuable for the wider applicability of metallic glasses in general.

Deformation in metallic glasses at temperatures below their glass transition ($T \ll T_g$) typically occurs through the formation of highly localized shear bands with a reduced viscosity compared to the bulk

material, intersecting the sample at around 45 ° [2]. The nucleation of these shear bands is thought to happen through the interaction of Shear Transformation Zones (STZ), atomic clusters with lower-than-average density, or higher-than-average free volume, and thus lower shear strength [3,4]. When sufficient elastic energy is stored in the material, cooperative interaction between the STZs will activate their topological coordination leading to the formation of shear bands with thicknesses typically in the order of 20 nm [5,6].

Shear banding is also often related to a localized rise in temperature [2,7–9]. It is thought that local temperature increase in the shear bands is not the primary cause of the viscosity drop, but a secondary effect of the localized plastic deformation [8]. Nevertheless, the increase in temperature may contribute to a further reduction of viscosity and destabilization of the shear bands [2]. The actual magnitude of the heating and its effects has been hotly debated, with answers depending on assumed adiabaticity, local deformation rate and shear band thickness [2,7]. The relation between shear banding as a deformation mode and temperature, has further put forward the obvious question of the effect of ambient temperature. Theoretical work on yield strength as a function of temperature has shown a good fit with experimental work, when normalized to the glass transition temperatures of different alloys [3,5,10]. Lowered temperature is generally predicted to increase strength. Several experimental studies have looked at different BMG alloys in cryogenic conditions, reporting increases in yield strength [11–13] and plasticity [11,12,14]. [Some report the concentration of deformation into one major shear band rather than several minor ones at low temperatures and strain rates \[10,15\].](#)

Though the operation of shear bands in metallic glasses, i.e. nucleation, propagation and arrest, is still not fully understood [2], intense research efforts in the last decade have improved our understanding of the deformation mechanisms and inspired novel strategies for designing BMGs with higher ductility. [For example, phenomena such as nanocrystallization in the shear bands \[16\], in-situ formation of soft crystalline phases in glassy matrices \[17\] and structural rejuvenation through thermal cycling \[18,19\] or thermomechanical processing \[20\] may provide promising routes for extending ductility in BMGs.](#) Yokoyama *et al.* [21] have shown that hypoeutectic bulk glass alloys have a promising potential for designing ductile BMGs, due to the higher free volume that can be quenched in during vitrification. Thus, designing a hypoeutectic $Zr_{70}Ni_{16}Cu_6Al_8$ BMG with high Poisson ratio (0.393 ± 0.003) and low Young's modulus (73 ± 4 GPa), plastic deformation positively correlated to strain rate in tensile mode was found, with a maximum of 1.7 % at $2 \times 10^{-1} s^{-1}$. The plasticity for this alloy was later improved to 2.8 % by increasing the sample cooling rate during casting, entrapping higher free volume to facilitate STZ coordination, as well as by testing at $1.5 \times 10^{-1} s^{-1}$ [22]. This improvement was linked to an increased ability to form multiple shear bands at high strain rates [14,22]. Low temperature and strain rate, i.e. 133 K and $10^{-4} s^{-1}$ respectively, were found to further increase the plastic deformability, but with a lower number of shear bands apparent on the surface [15].

In the present work, the hypoeutectic $Zr_{70}Ni_{16}Cu_6Al_8$ bulk glassy alloy was tested in tension at various strain rates, nominally 10^{-4} , 10^{-3} , 10^{-2} and $10^{-1} s^{-1}$. Ambient temperature was set to 77 K, 150 ± 20 K (referred to as “150 K” from now on) and 295 K during the tests in order to evaluate the effect of strain rate and low temperature on the mechanical behaviour of BMGs and gain new insights on the deformation mechanism. The samples were filmed during the tensile tests using a high frame rate camera, allowing the direct observation of the deformation phenomena and how they are affected by the imposed conditions.

Experimental Procedure

Zr₇₀Ni₁₆Cu₆Al₈ master alloy ingots were produced by weighing out in total 30 g of alloying elements to within an error of 1 %. The ingots were automatically melted, flipped and remelted four times in a Diavac Limited arc melter under 5N Ar atmosphere.

A Nissin Giken double torch arc melter and tilt casting system[23] was used to cast cylindrical rods with 3.5 mm diameter and 85 mm length. All castings were done under 5N Ar protective atmosphere using Zr as oxygen getter. The rods were individually verified to be amorphous using a Rigaku Ultima IV X-ray diffractometer. 28 mm long tensile specimens with a 2.3 by 0.8 mm gage area with circular cross section were machined from the cast rods. All samples were polished with 4000 grit lapping tape and checked for surface defects using a Shimadzu HMV-2 ADW optical microscope.

Tensile testing was performed at nominal strain rates of 10^{-1} , 10^{-2} , 10^{-3} and 10^{-4} s⁻¹ at 295 K, 150 K and 77 K. Tests at 77 K were done submerged in liquid nitrogen, while the intermediate temperature was achieved by suspending the sample above the liquid nitrogen surface. A specially designed sample holder for liquid nitrogen submersion was used on a strain rate controlled Shimadzu AG-X tensile testing machine. [Specimen temperature was measured by a thermocouple attached to the sample holder.](#) Two specimens were tested for each combination of strain rate and temperature.

[The tensile tests were filmed using a Photron FASTCAM SA1.12 high speed camera with a Leica Z16 APO lens at framerates between 60 and 5400 frames per second \(depending on strain rate\). The strain data was measured both by cross-beam displacement and through Digital Image Correlation\(DIC\) using eCorr software by Egil Fagerholt and Track Eye Motion Analysis software by Imagesystems \[24,25\]. Young's modulus was found by linear regression of DIC data. Stress-strain curves were constructed by combining the regressed elastic regime with plastic deformation data from the cross-beam displacement, smoothed and scaled to correct for machine compliance. This was done to compensate for high deformability in the special sample holder and for scatter in the DIC results.](#) High compliance in the sample holder required for liquid nitrogen submersion, resulted in only about 20 % of the applied nominal strain rate being transferred to the sample. The nominal strain rates are still used as reference for the remainder of the article.

Results and Discussion

The mechanical behaviour of the Zr₇₀Ni₁₆Cu₆Al₈ BMG under uniaxial tensile loading was investigated at temperatures between 295 K and 77 K using various nominal strain rates in the range from 10^{-4} s⁻¹ to 10^{-1} s⁻¹. Representative engineering stress-strain curves obtained at various temperatures for strain rates of 10^{-4} and 10^{-2} s⁻¹, are presented in Figure 1. It is interesting to note the effect on tensile behaviour of the Zr-based hypoeutectic BMG at cryogenic temperatures. The plastic strain increases from a negligible value at 295 K to 3.7% at 150 K, whereas at even lower temperatures (77 K) the plastic strain before fracture is in the order of 2%. These values of plastic deformation at cryogenic temperatures are remarkable for BMGs, which are known to exhibit very limited plastic strains under tensile loading. In addition, a clear increase of the mechanical strength can be observed from about 1400 MPa at 295 K to 1700 MPa at 77 K.

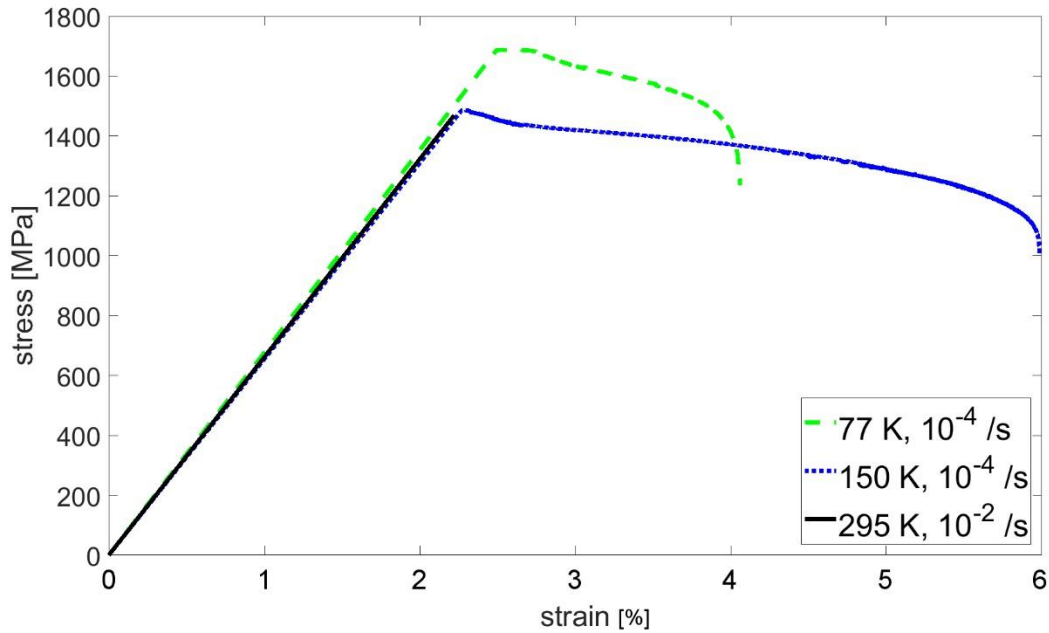


Figure 1: Representative stress-strain curves for samples tested at 10^{-4} and 10^{-2} s⁻¹ nominal strain rate at 77, 150 and 295 K.

Figure 2 a) and b) show the yield stress and tensile plastic deformation before fracture, respectively, as a function of temperature for the various strain rates used in the present work. Each value in these graphs represents the average of two independent experiments, whereas the error bars indicate the highest and lowest measurements in the group. The dispersion of values in the yield strength and ductility, indicated by the error bars in Figure 2 a) and b) respectively, is firstly noted. Such dispersion may not be surprising for the tensile properties of BMGs and may be related to the sensitivity of their mechanical behaviour to nano- and micro-scale defects, as well as local structural variations introduced during casting. Therefore, for the remainder of the present work, focus is on the main clear trends observed in the graphs rather than the absolute values.

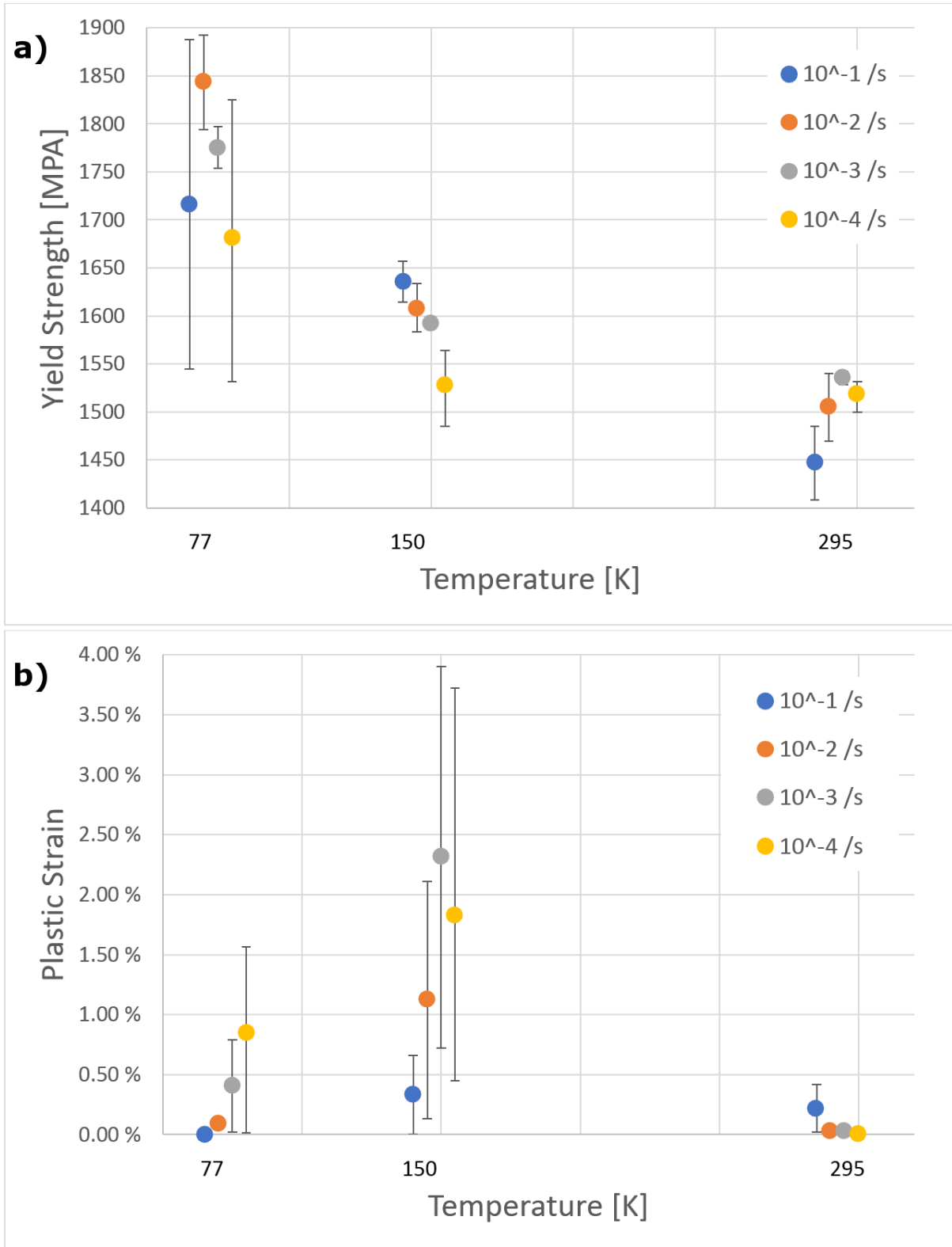


Figure 2: Comparison of tensile mechanical properties for the $Zr_{70}Ni_{16}Cu_6Al_8$ BMGs for various strain rates ranging between 10^{-1} to $10^{-4} s^{-1}$ at 77, 150 and 295 K: a) Yield strength as a function of temperature and b) Plastic strain before fracture as a function of temperature. Error bars mark highest and lowest measured values.

In Figure 2 a) the tensile yield strength, σ_y , is observed to increase with decreasing temperature for all the strain rates used in this work. This increase in the yield strength is in the order of 10-15 % from 295 K to 77 K, in good agreement with the strengthening of BMGs at cryogenic temperatures

reported in the literature [5,10–13,26]. It has been proposed that the strengthening at cryogenic temperatures may be attributed to structural densification related with the reduction of atomic radii through the reduction of thermal atomic fluctuations and to increased bond strengths at low temperatures [5,11–13,26]. In addition, such behaviour may be related to the reduced mobility of STZs, which are thermally hindered from assuming positions conducive to cooperative shear [12]. Between 150 and 295 K, there happens an apparent reversal of strain rate sensitivity with regards to yield stress. Maass *et al.* showed a good fit for positive correlation with strain rate below a critical temperature (approximated to 200 K for the similar Vit105 alloy) [10], drawing the analogy to non-Newtonian flow in viscous media. For compressive deformation, the disappearance of flow serration was reported at the same temperature, along with a reversal of strain rate sensitivity. This was explained by structural rejuvenation around the STZ when sufficient thermal energy and time is supplied[27].

Figure 2 b) shows the tensile plastic elongation of $Zr_{70}Ni_{16}Cu_6Al_8$ as a function of temperature for the strain rates used in the present work. Interestingly, the hypoeutectic Zr-based BMG exhibits (limited but appreciable) room temperature ductility at higher strain rates ($\sim 10^{-1} s^{-1}$), whereas no plastic deformation was observed at lower strain rates 10^{-2} - $10^{-4} s^{-1}$. The absence of tensile plastic deformation at low strain rates and the ductility at high strain rates is in general agreement with previous observations by Yokoyama *et al.*[22]. It has to be noted, however, that the tensile elongation at room temperature and high strain rates observed in the present work is lower than that observed by Yokoyama *et al.* [22], which may be related to the sensitivity of the tensile behaviour of BMGs to the manufacturing processes as well as to variations in machine compliance. More interestingly, increased tensile ductility can be observed at 150 K for all the strain rates, reaching a remarkable 2.4% average plastic strain at $10^{-3} s^{-1}$ strain rate, despite the observed dispersion of measured values. At even lower temperature, 77 K, the tensile ductility decreases again but maintains appreciable plastic deformation values of the order of 0.8% and 0.4% at $10^{-4} s^{-1}$ and $10^{-3} s^{-1}$ strain rates respectively. Change in plastic deformability at low temperatures has been previously reported at various magnitudes. Dependent on alloy composition, improvements in plastic tensile deformability at cryogenic temperatures have ranged from none [13], through less than one percent [11,12] to several percent [15] for Zr-based BMGs. Lower strain rate gives higher plasticity for both cryogenic temperatures, which could relate to the change from a Newtonian to non-Newtonian regime in the stress-strain rate-temperature relationship of the viscosity in the sliding shear band.

Figure 3 a), b) and c) shows images recorded in-situ by a high-speed camera during the tensile test of the Zr-based BMG (at 295 K and $10^{-1} s^{-1}$ strain rate) at progressive stages of deformation, while Figure 3 d) shows a zoom-in at the plastic deformation region of the corresponding stress-strain curve. As can be seen from Figure 3 a) a shear step formed on the surface of the tensile specimen about 35 ms before fracture as a result of a shear band operating in a cross-sectional plane. Figure 3 b) shows the formation of a second shear step in close proximity, eventually intersecting the first shear band. After intersection, the specimen enters a new elastic-like linear regime before fracture finally occurs through the second shear band as seen in Figure 3 c). In the present work, tensile plasticity at room temperature was only observed when two (or more) shear bands nucleated to intersect each other, as shown in Figure 3 b) and c). Tensile plastic deformation at room temperature occurs through the formation of multiple shear bands; thus, the operation of a higher number of shear bands increases the recorded plastic deformation and increases the probability of interacting with each other. The formation of multiple shear bands during tensile loading provokes the serrated flow observed in Figure 3 d), resembling the serrated flow observed under compressive loads[9,28]. The temporal resolution to deeply study flow serrations was however not available on

the used setup. Previous work [15] found a positive correlation between absolute number of shear bands observed on the sample surface and strain rate, suggesting a higher deformability at higher strain rates, supporting the present observations.

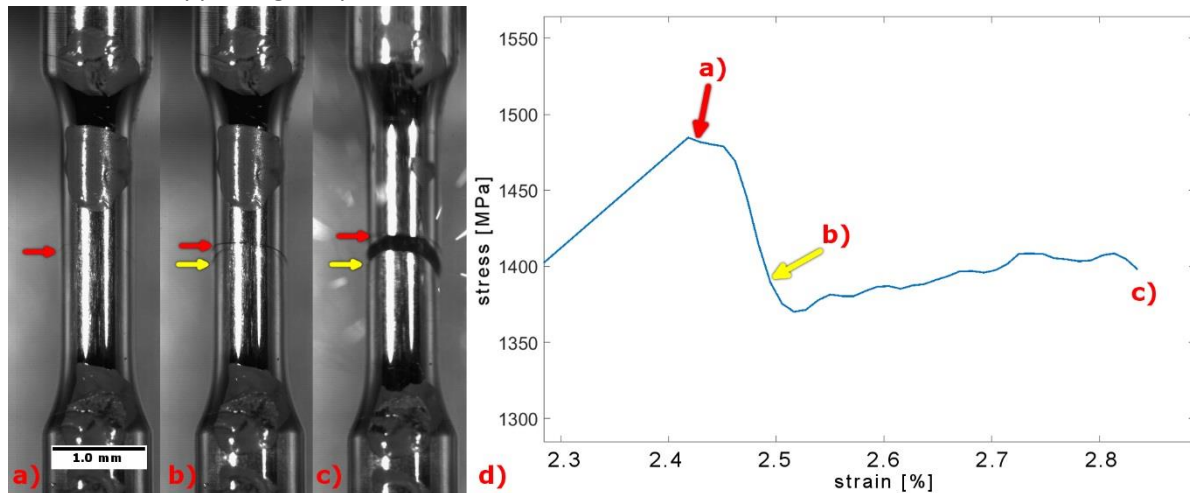


Figure 3: Nucleation of intersecting shear bands at 295 K, 10^{-1} s^{-1} nominal strain rate. a) first shear band, red arrow, appears 35 ms before fracture, b) second shear band, yellow arrow, nucleates to intersect first shear band at 30 ms before fracture and c) final fracture along second shear band.

On the other hand, even though higher tensile ductility was observed at cryogenic temperatures as shown in Figure 1 and Figure 2 b), plastic deformation was accommodated mainly through the operation of a single shear band. Figure 4 a) through c) shows images of the evolution of plastic deformation for $\text{Zr}_{70}\text{Ni}_{16}\text{Cu}_6\text{Al}_8$ during tension under tensile loading at 150 K and 10^{-4} s^{-1} strain rate. Figure 4 a) shows the initial stages of formation of a large shear step at the surface of the tensile specimen resulting from the operation of one shear band. As can be seen the shear step forms at the beginning of the yield flow as indicated in Figure 4 d). Plastic deformation in this case mainly occurs through the propagation of this main shear band which remarkably accommodates more than 3% plastic strain before fracture, see Figure 4 b) and c). In the case of tests run at 10^{-4} s^{-1} strain rate, the whole shear event of the major shear band elapsed over the order of tens of seconds, and can therefore be regarded as truly stable plastic flow. The sliding of shear bands can be regarded as exothermic, with the added heat further amplifying the instability of structurally reduced viscosity[7]. At low strain rate and low temperature, both time and driving force are supplied to allow heat to diffuse out from the shear band. This might be enough to delay the final stage of critical failure, letting the viscous layer slide in a stable manner before runaway instability.

Comparison of SEM investigations of fracture and lateral surfaces with what was captured by the recorded videos reveals that the specimens do in fact show nucleation of several minor shear bands, as well as sliding of the primary band. Figure 5 shows representative micrographs at room temperature, a) and b), and liquid nitrogen, c) and d), tests. Evidence of the sliding shear band is marked by lines on the fracture surfaces in Figure 5 a) and c). In the videos, the sliding can only be observed at low temperatures except for the single case shown in Figure 5. This difference in timeframe, sliding and rupture in only the range of milliseconds at high temperature and over minutes at low temperatures indicates a difference in its role in deformation. At high temperature, sliding is catastrophic and cannot be stopped. Although the fracture morphology left behind is similar, the sliding at low temperature is slow and can be arrested by unloading[10], and can therefore be regarded as true plasticity. In some cases, only a single shear band nucleated, to accommodate the entire strain, while in most cases a major shear band was selected from among many nucleated ones. This has similarly been observed in both compression [10] and tension [15],

where the single shear banding can be related to the presence of defects that induce shear before normally expected flow stress is reached.

Interestingly, tests at 77 K exhibit lower plastic capacity than those at 150 K. In this case deformation still mainly occurs through the operation of the primary shear band, similar to what is observed at 150K, see Figure 4.

A linear decrease in impact toughness with decreasing temperature has previously been observed for some metallic glasses [29] which could impact plastic deformability as a competition between embrittlement and shear band stabilization. Reduced mobility of STZs could likewise be a factor in the re-lowering of plasticity at 77K. If low-temperature deformation is purely driven by STZ coalescence, lower diffusivity could inhibit their ability to accommodate strain, resulting in a more brittle failure.

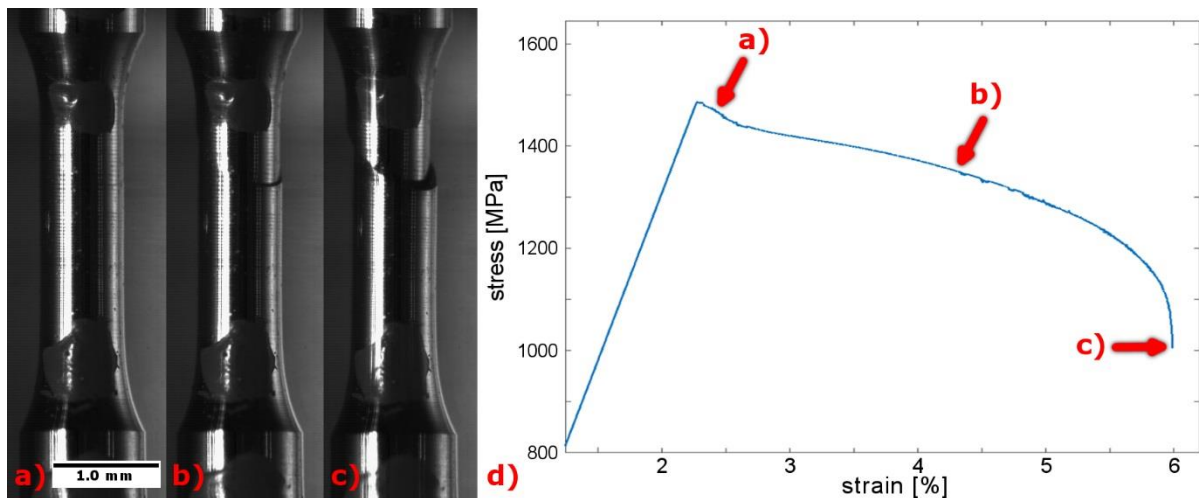


Figure 4: Nucleation and propagation of single shear band in stable flow at 150 K, 10^{-4} s^{-1} nominal strain rate. a) first trace of shear band 80 s before fracture, b) extent of shear band flow 38 s before fracture and c) final video frame at the time of fracture.

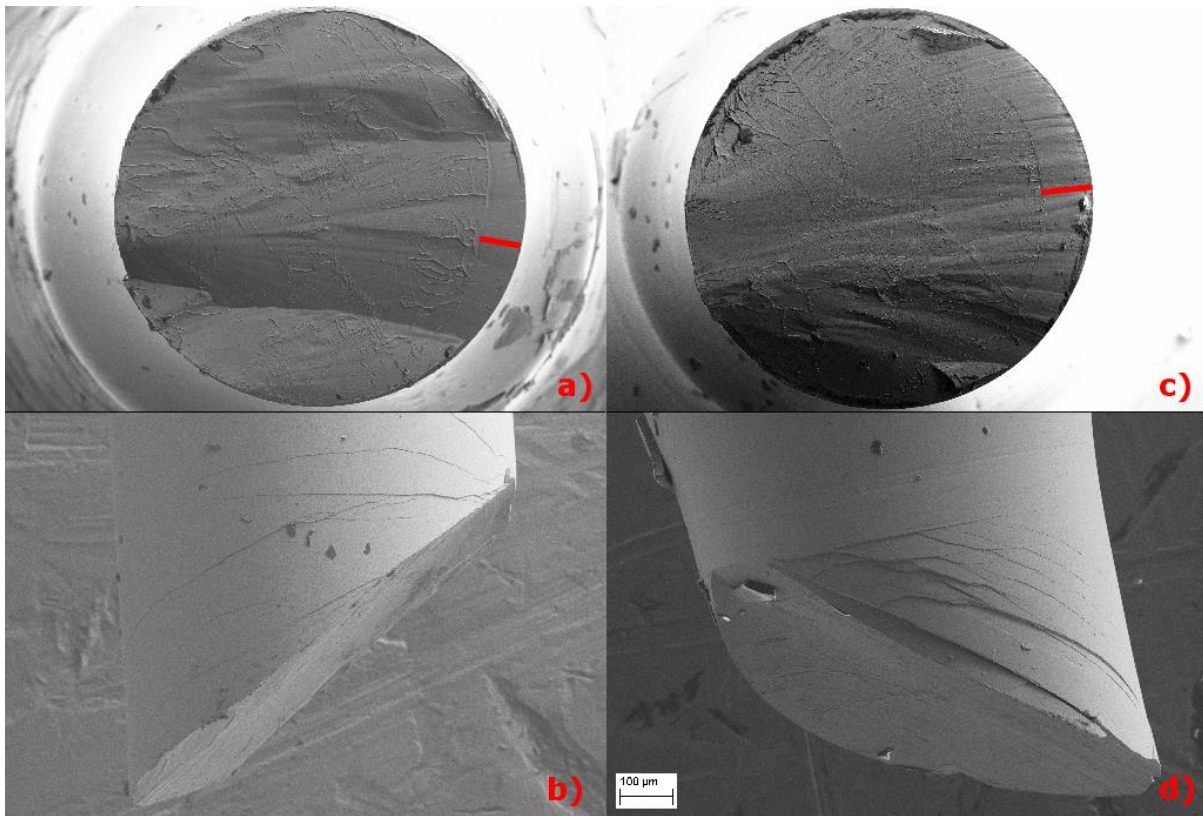


Figure 5: SEM micrographs of fracture surfaces, top, and lateral surfaces, bottom, of samples tested at room temperature, a) and b), and in liquid nitrogen, c) and d). Sliding of the primary shear band marked by red lines in a) and b). In a) the intersection of two major shear bands, previously shown in Figure 3 can also be seen. (The spots on the sample surface are remainders of marks used for DIC)

Conclusion

The tensile mechanical behaviour of a $Zr_{70}Ni_{16}Cu_6Al_8$ BMG was investigated at room and cryogenic temperatures using four different nominal strain rates in the range between 10^{-4} and $10^{-1} s^{-1}$. The yield strength was found to increase at lower temperatures, ranging from a 1503 MPa average at room temperature to 1746 MPa at 77 K. A reversal of strain rate sensitivity was observed between 150 and 295 K, where low strain rate at room temperature and high strain rate at low temperatures resulted in the highest observed yield strengths. Plastic deformation was found to increase at lower temperatures compared to room temperature. However, tensile ductility does not increase monotonically with decreased temperature; the highest plastic strains were observed at 150 K for all the strain rates reaching an average 2.4% at $10^{-3} s^{-1}$, which is remarkable for tensile loading of BMGs. Different mechanisms of apparent plasticity were observed at room and cryogenic temperatures. Tensile plastic deformation at room temperature occurs through the formation of multiple shear bands, whereas at lower temperatures (150 K and 77 K) deformation mainly happens through the operation of a single shear band. The high plastic deformability at lower temperatures and strain rates is thought to stem from the temperature dependence of the Newtonian-non-Newtonian flow transition as well as the reduced adiabaticity of the shear bands due to both an increased driving force and longer allowed time for heat dissipation, allowing a single preferred shear band to deform in a stable manner. At the same time, competition with linearly dropping fracture toughness with a decrease in temperature is thought to contribute to higher plasticity at intermediate temperature than at liquid nitrogen temperature.

Funding

This work was supported by the Department of Materials Science and Engineering, Norwegian University of Science and Technology (NTNU), Trondheim, Norway, and the Institute of Materials Research, Tohoku University, Sendai, Japan.

References

- [1] M. Ashby, A.L. Greer, Metallic glasses as structural materials, *Scr. Mater.* 54 (2006) 321–326. doi:10.1016/j.scriptamat.2005.09.051.
- [2] A.L. Greer, Y.Q. Cheng, E. Ma, Shear bands in metallic glasses, *Mater. Sci. Eng. R Reports.* 74 (2013) 71–132. doi:10.1016/j.mser.2013.04.001.
- [3] A.. Argon, Plastic deformation in metallic glasses, *Acta Metall.* 27 (1979) 47–58. doi:10.1016/0001-6160(79)90055-5.
- [4] F. Spaepen, Homogeneous flow of metallic glasses: A free volume perspective, *Scr. Mater.* 54 (2006) 363–367. doi:10.1016/j.scriptamat.2005.09.046.
- [5] W.L. Johnson, K. Samwer, A Universal Criterion for Plastic Yielding of Metallic Glasses with a $(T/T_g)^{2/3}$ Temperature Dependence, *Phys. Rev. Lett.* 95 (2005) 195501. doi:10.1103/PhysRevLett.95.195501.
- [6] A.R. Yavari, K. Georgarakis, W.J. Botta, A. Inoue, G. Vaughan, Homogenization of plastic deformation in metallic glass foils less than one micrometer thick, *Phys. Rev. B.* 82 (2010) 172202. doi:10.1103/PhysRevB.82.172202.
- [7] J.J. Lewandowski, A.L. Greer, Temperature rise at shear bands in metallic glasses, *Nat. Mater.* 5 (2006) 15–18. doi:10.1038/nmat1536.
- [8] F. Spaepen, Metallic glasses: Must shear bands be hot?, *Nat. Mater.* 5 (2006) 7–8. doi:10.1038/nmat1552.
- [9] K. Georgarakis, M. Aljerf, Y. Li, A. LeMoulec, F. Charlot, A.R. Yavari, K. Chornokhvestenko, E. Tabachnikova, G.A. Evangelakis, D.B. Miracle, A.L. Greer, T. Zhang, Shear band melting and serrated flow in metallic glasses, *93* (2008) 31907. doi:10.1063/1.2956666.
- [10] R. Maaß, D. Klaumünzer, E.I. Preiß, P.M. Derlet, J.F. Löffler, Single shear-band plasticity in a bulk metallic glass at cryogenic temperatures, *Scr. Mater.* 66 (2012) 231–234. doi:10.1016/j.scriptamat.2011.10.044.
- [11] L.S. Huo, H.Y. Bai, X.K. Xi, D.W. Ding, D.Q. Zhao, W.H. Wang, R.J. Huang, L.F. Li, Tensile properties of ZrCu-based bulk metallic glasses at ambient and cryogenic temperatures, *J. Non. Cryst. Solids.* 357 (2011) 3088–3093. doi:10.1016/j.jnoncrysol.2011.04.017.
- [12] Y.H. Li, W. Zhang, C. Dong, A. Kawashima, A. Makino, P.K. Liaw, Effects of cryogenic temperatures on mechanical behavior of a Zr60Ni25Al15 bulk metallic glass, *Mater. Sci. Eng. A.* 584 (2013) 7–13. doi:10.1016/j.msea.2013.06.063.
- [13] J. Yi, S.M. Seifi, W. Wang, J.J. Lewandowski, A Damage-tolerant Bulk Metallic Glass at Liquid-nitrogen Temperature, *J. Mater. Sci. Technol.* 30 (2014) 627–630. doi:10.1016/j.jmst.2014.04.017.
- [14] H. Tokunaga, Y. Nitta, A. Shirota, K. Fujita, Y. Yokoyama, T. Yamasaki, A. Inoue, Tensile Plastic Deformation of Zr 70 Ni 16 Cu 6 Al 8 Bulk Metallic Glass at Cryogenic Temperature, *J. Japan Inst. Met.* 73 (2009) 919–923. https://www.jstage.jst.go.jp/article/jinstmet/73/12/73_12_919/_pdf (accessed June 6,

- 2017).
- [15] H. Tokunaga, K. Fujita, Y. Yokoyama, Tensile Plastic Deformation Behavior of Zr 70 Ni 16 Cu 6 Al 8 Bulk Metallic Glass at Cryogenic Temperature, (n.d.). doi:10.2320/matertrans.M2012102.
- [16] A.R. Yavari, K. Georgarakis, J. Antonowicz, M. Stoica, N. Nishiyama, G. Vaughan, M. Chen, M. Pons, Crystallization during Bending of a Pd-Based Metallic Glass Detected by X-Ray Microscopy, *Phys. Rev. Lett.* 109 (2012) 85501. doi:10.1103/PhysRevLett.109.085501.
- [17] S. Pauly, S. Gorantla, G. Wang, U. Kühn, J. Eckert, Transformation-mediated ductility in CuZr-based bulk metallic glasses., *Nat. Mater.* 9 (2010) 473–477. doi:10.1038/NMAT2767.
- [18] S. V Ketov, Y.H. Sun, S. Nachum, Z. Lu, A. Checchi, A.R. Beraldin, H.Y. Bai, W.H. Wang, D. V Louzguine-Luzgin, M.A. Carpenter, A.L. Greer, Rejuvenation of metallic glasses by non-affine thermal strain, (n.d.). doi:10.1038/nature14674.
- [19] W. Guo, R. Yamada, J. Saida, Rejuvenation and plasticization of metallic glass by deep cryogenic cycling treatment, *Intermetallics.* 93 (2018) 141–147. doi:10.1016/j.intermet.2017.11.015.
- [20] Y. Sun, A. Concustell, A.L. Greer, Thermomechanical processing of metallic glasses: extending the range of the glassy state, *Nat. Rev. Mater.* 1 (2016) 16039. doi:doi:10.1038/natrevmats.2016.39.
- [21] Y. Yokoyama, K. Fujita, A.R. Yavari, A. Inoue, Malleable hypoeutectic Zr–Ni–Cu–Al bulk glassy alloys with tensile plastic elongation at room temperature, *Philos. Mag. Lett.* 89 (2009) 322–334. doi:10.1080/09500830902873575.
- [22] Y. Yokoyama, H. Tokunaga, A.R. Yavari, T. Kawamata, T. Yamasaki, K. Fujita, K. Sugiyama, P.K. Liaw, A. Inoue, Tough Hypoeutectic Zr-Based Bulk Metallic Glasses, *Metall. Mater. Trans. A.* 42A (2011) 1468–1475. doi:10.1007/s11661-011-0631-1.
- [23] Y. Yokoyama, K. Inoue, K. Fukaura, Pseudo Float Melting State in Ladle Arc-Melt-Type Furnace for Preparing Crystalline Inclusion-Free Bulk Amorphous Alloy, *Mater. Trans.* 43 (2002) 2316–2319. doi:10.2320/matertrans.43.2316.
- [24] E. Fagerholt, Field measurements in mechanical testing using close-range photogrammetry and digital image analysis, Norwegian University of Science and Technology, 2012. http://folk.ntnu.no/egilf/Thesis_Egil_Fagerholt.pdf (accessed June 15, 2017).
- [25] S.X. Song, X.-L. Wang, T.G. Nieh, Capturing shear band propagation in a Zr-based metallic glass using a high-speed camera, *Scr. Mater.* 62 (2010) 847–850. doi:10.1016/j.scriptamat.2010.02.017.
- [26] R. Maaß, J.F. Löffler, Shear-Band Dynamics in Metallic Glasses, *Adv. Funct. Mater.* 25 (2015) 2353–2368. doi:10.1002/adfm.201404223.
- [27] A. Dubach, F.H. Dalla Torre, J.F. Löffler, Deformation kinetics in Zr-based bulk metallic glasses and its dependence on temperature and strain-rate sensitivity, *Philos. Mag. Lett.* 87 (2007) 695–704. doi:10.1080/09500830701494037.
- [28] B.A. Sun, S. Pauly, J. Tan, M. Stoica, W.H. Wang, U. Kühn, J. Eckert, Serrated flow and stick-slip deformation dynamics in the presence of shear-band interactions for a Zr-based metallic glass, *Acta Mater.* 60 (2012) 4160–4171. doi:10.1016/j.actamat.2012.04.013.
- [29] S. Roberts, C. Zachrisson, H. Kozachkov, A. Ullah, A.A. Shapiro, W.L. Johnson, D.C. Hofmann, Cryogenic Charpy impact testing of metallic glass matrix composites, *Scr. Mater.* 66 (2012) 284–287. doi:10.1016/j.scriptamat.2011.11.011.

Captions

Figure 1: Representative stress-strain curves for samples tested at 10^{-4} and 10^{-2} s $^{-1}$ nominal strain rate at 77, 150 and 295 K.

Figure 2: Comparison of tensile mechanical properties for the $Zr_{70}Ni_{16}Cu_6Al_8$ BMGs for various strain rates ranging between 10^{-1} to 10^{-4} s $^{-1}$ at 77, 150 and 295 K: a) Yield strength as a function of temperature and b) Plastic strain before fracture as a function of temperature. Error bars mark highest and lowest measured values.

Figure 3: Nucleation of intersecting shear bands at 295 K, 10^{-1} s $^{-1}$ nominal strain rate. a) first shear band, red arrow, appears 35 ms before fracture, b) second shear band, yellow arrow, nucleates to intersect first shear band at 30 ms before fracture and c) final fracture along second shear band.

Figure 4: Nucleation and propagation of single shear band in stable flow at 150 K, 10^{-4} s $^{-1}$ nominal strain rate. a) first trace of shear band 80 s before fracture, b) extent of shear band flow 38 s before fracture and c) final video frame at the time of fracture.

Figure 5: SEM micrographs of fracture surfaces, top, and lateral surfaces, bottom, of samples tested at room temperature, a) and b), and in liquid nitrogen, c) and d). Sliding of the primary shear band marked by red lines in a) and b). In a) the intersection of two major shear bands, previously shown in Figure 3 can also be seen. (The spots on the sample surface are remainders of marks used for DIC)